Nat Hazards (2015) 76:41–61
DOI 10.1007/s11069-014-1480-1

ORIGINAL PAPER

Re-assessing volcanic hazard zonation of Volcán de Colima, México

L. Capra · J. C. Gavilanes-Ruiz · R. Bonasia · R. Saucedo-Giron · R. Sulpizio

Received: 17 March 2014 / Accepted: 14 October 2014 / Published online: 25 October 2014

Abstract Volcán de Colima is one of the most active volcanoes in Mexico. Several hazard maps have been published based on reconstruction of the Late Pleistocene–Holocene eruptive history and historical records for the last 400 years. Recent detailed published studies have improved the knowledge of the eruptive history of the volcano and proposed a new hazard zonation based on numerical simulation for debris avalanche, pyroclastic density currents (PDCs), debris flows and fallout events. The new hazard map incorporates all these new data and proposes a revised hazard zonation useful for improving decision-making both previously and during crises. A sub-Plinian to Plinian multi-stage eruption similar to the AD 1913 event would represent a major hazard for populated areas around Volcán de Colima. PDCs initiated by column collapses could travel up to 15 km from the eruptive vent. Tephra dispersal modeling shows that up to 10 cm of fallout deposits could affect several cities (population more than ~180,000 people). Lahars (including the wide spectra of volcaniclastic flows), the most common hazard during the rainy season, would affect the main ravines up to a distance of 15 km from the Volcán de Colima cone, impacting infrastructures and small villages. A Plinian eruption scenario also includes the possible generation of large volume lahars (up to 5×10^6 m^3), possibly reaching major villages (i.e., San Marcos, Quesería, Tonila) with catastrophic effects. Block-and-ash PDCs from summit dome collapse will travel in the main ravines up to distances between 4 and 7 km, with slightly longer runout for associated turbulent PDCs. Despite a recurrence rate probably >2,000 years, partial

L. Capra (✉) · R. Bonasia
Centro de Geociencias, Campus Juriquilla, UNAM, Querétaro, Mexico
e-mail: lcapra@geociencias.unam.mx

J. C. Gavilanes-Ruiz
Licenciatura en Ciencia Ambiental y Gestión de Riesgos, Facultad de Ciencias, Universidad de Colima, Colima, Mexico

R. Saucedo-Giron
Instituto de Geología, Universidad Autónoma de San Luis Potosí, San Luis Potosí, Mexico

R. Sulpizio
Dipartimento di Scienze della Terra e Geoambientali, via Orabona 4, 70125 Bari, Italy

edifice collapse constitutes the major hazard. Large volume (>5 km^3) debris avalanches can disrupt the southern slopes of the volcano up to a distance of 30 km affecting the Colima city, potentially associated with laterally directed blasts and secondary debris flows that in the past reached the Pacific coast.

Keywords Volcán de Colima · Volcanic hazard · Numerical simulation

1 Introduction

Volcán de Colima is one of the most active volcanoes in Mexico (Fig. 1a). At present (September 2014), after 3 years of dome growing, the explosive activity renewed with small explosions and the emplacement of rock falls and small pyroclastic density currents (PDCs) down to 3 km from the summit dome. The 1913 Plinian eruption is the largest event in the last century and was characterized by the emplacement of several scoria/pumice flows and fallout dispersal to the NE (Saucedo et al. 2010). Other Plinian eruptions were reported in AD 1818 and probably in AD 1690 (Luhr and Carmichael 1982). After the AD 1913 eruption, the volcano experienced several volcanic crises initiated by dome growth and successive collapses. The Holocenic tephro-stratigraphic record is incomplete due to low preservation of tephra in tropical climate (Luhr et al. 2010), but also for the erosive effects of the subsequent volcanic events (i.e., lahars). In contrast, the Holocene and Late Pleistocene eruptive records activity of Volcán de Colima and its ancestral edifice, the Paleofuego Volcano, indicate that volcanic collapses represented a recurrent activity, with partial or total destruction of the edifice and the emplacement of large volume (1–18 km^3) debris avalanche deposits, including the 7,500 year. BP debris avalanche on top of which the cities of Colima and Villa de Alvarez are edified (Komorowski et al. 1997).

To date, two main hazard maps have been published (Del Pozzo et al. 1996; Navarro and Cortés 2003), both based on the stratigraphic record of past eruptions. Since then, a detailed analysis of eruptive activity of the Volcán de Colima have been presented by several authors, including the detailed stratigraphic reconstruction of past events, definition of magnitude and aerial distribution of deposits, and hazard assessment based on numerical simulations for different eruptive scenarios (Saucedo et al. 2005; Dávila et al. 2007; Saucedo et al. 2008, 2010; Cortés et al. 2010a, b; Sulpizio et al. 2010; Bonasia et al. 2011; Borselli et al. 2011; Capra et al. 2014). The purpose of this paper is to present a revised volcanic hazard zonation for the Volcán de Colima that benefits from all these new works including the geological map of the volcano (Cortés et al. 2010a), and the hazard zonation based on numerical simulations (i.e., Saucedo et al. 2005; Dávila et al. 2007; Sulpizio et al. 2010; Bonasia et al. 2011). These previous works are here synthesized and adapted to propose: (1) hazard zonation for different eruptive scenarios (sub-Plinian/Plinian eruption, dome grown/collapse, edifice failure, rain-triggered lahars); (2) a qualitative hazard map where all these hazards are superimposed; and finally (3) a susceptibility map, where zone more prone to be affected by a volcanic event are identified, and hazard is ranked using a color scale.

2 Eruptive history of Volcán de Colima

Volcán de Colima is the youngest and active volcano of the Colima Volcanic Complex and consists of the ancestral edifice named Paleofuego, and the active cone, also known as

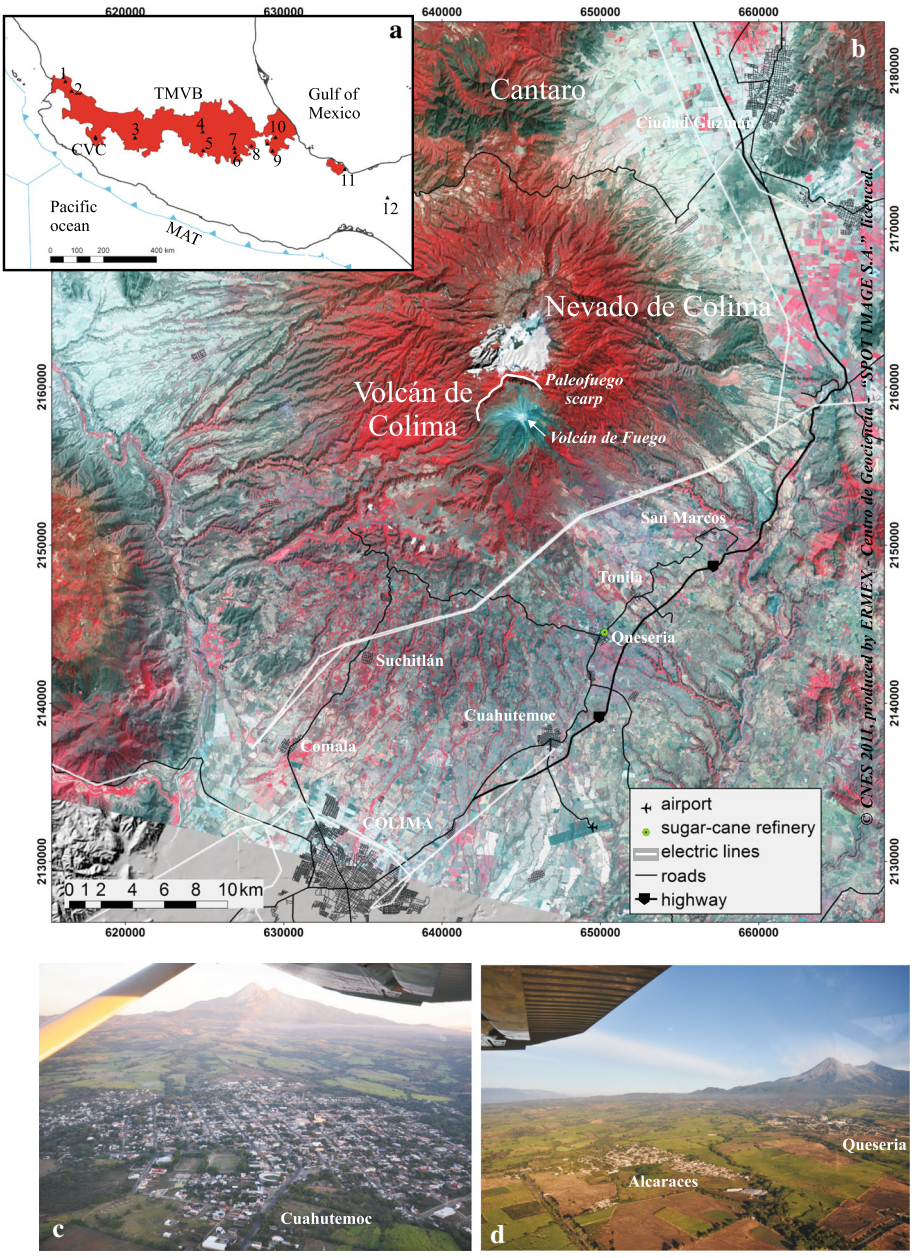

Fig. 1 **a** Sketch map of the Trans-Mexican Volcanic Belt where the Colima Volcanic Complex and other main stratovolcanoes are located: *1* San Juan; *2* Ceboruco; *3* Tancitaro; *4* Jocotitlán; *5* Nevado de Toluca; *6* Popocatépetl; *7* Ixtacíhuatl; *8* La Malinche; *9* Pico de Orizaba; *10* Cofre de Perote; *11* San Martín; *12* Chichón. **b** spot image (1, 2 and 3 bands in RGB combination, 10 m of resolution) showing the Colima Volcanic Complex, with the Volcán de Colima edifice that consists of the active Volcán de Fuego cone built inside the Paleofuego scarp (*white line*). Aerial view of the southern sector of the Volcán de Colima showing the main towns (**c**, Cuahutémoc and **d**, Quesería and Alcaraces) which are surrounded by extensive cultivated fields

Volcán de Fuego, that is built inside the Paleofuego caldera, a scarp formed from an edifice failure event (Fig. 1b). The age of the active cone has been estimated at about 2,500 year BP that corresponds with the age of the last edifice failure (Komorowski et al. 1997) (Table 1). One of the main debates is about the origin and age of the Paleofuego caldera. Luhr and Prestegaard (1988) and Robin et al. (1987), both consider that this scarp is the product of a single event, occurred 4,280 ± 180 year BP or 9,370 ± 400 year BP, respectively. Komorowski et al. (1997) point out the possibility that the scarp is the result of several discrete collapses, based on the evidence of the presence of at least nine different debris avalanche deposits that can be recognized on the southern sector of the volcano (Table 1). Roverato et al. (2011) proposed that the Paleofuego scarp is probably Pleistocenic in age. These uncertainties are mainly related to the difficulty in correlating debris avalanche outcrops around the volcano, mostly because of the lack of outcrops exposing stratigraphic relations, the homogenous composition of the lava fragments, being all andesitic, and finally the difficulty in correlating the deposits with their source area. Despite these uncertainties, it is clear that edifice failure has been a recurrent event at Colima. Minor eruptive episodes have not been identified in the Late Pleistocene eruptive records of Volcán de Colima probably eroded and buried by the voluminous debris avalanche deposits.

A detailed study about the Holocene stratigraphic record of Volcán de Colima (Luhr et al. 2010) identified a period of high explosive activity between 3,000 and 4,000 year. BP and between 500 and 1,500 year. BP, but the low preservation of the studied deposits has made it very difficult to reconstruct the characteristics and magnitude of these eruptions. In contrast, a quite good historic record for the Volcán de Fuego active cone for the last 500 years is available (Table 2) (De la Cruz-Reyna 1993; Breton et al. 2002). During the last 5 centuries, the most violent Plinian eruptions occurred in AD 1576, AD 1818 and AD 1913, sub-Plinian events were also reported in AD 1622 and AD 1711 (Table 2). For the older episodes, no detailed data are available, but the 1913 activity was well documented and studied (Saucedo et al. 2010; Gavilanes-Ruiz and Cuevas-Muñiz 2014). The AD 1869 activity is quite distinctive; it started on the NE flank of the volcano and gave place to the formation of El Volcancito scoria cone and associated lava flows that lasted up to AD 1878 and was accompanied by several eruptive columns up to 4,000 m in height. The AD 1913 Plinian eruption represents the largest known historic eruption of this volcano, with the formation of a 23-km-high eruptive column, whose products directly affected the western and central regions of Mexico. After this cataclysmic event, Volcán de Colima experienced several volcanic crises. Examples are the AD 1991, 1994, 1998–1999 and 2004–2005 events, characterized by a rapid dome growth (few months) and subsequent gravitational collapse or associated with strong explosions (Merapi and Soufriere type). The associated block-and-ash PDCs emplaced on main ravines down to a maximum of 6.1 km from the summit. The more diluted ash clouds traveled up to few hundred meters farther downslope. Lava flows were also erupted. In AD 1975, three lava flows emplaced on the SE flank of the volcano, down to a distance of 4,500 m, and in AD 2004 a lava flow extruded from the crater and partially filled the El Playón, the depression confined by the Paleofuego scarp. Lahars have been recognized all along the stratigraphic record of the volcano, from very large debris flows linked to major edifice collapse events (Cortés et al. 2010a, b) to post-eruptive lahars associated to Plinian or dome-collapse eruptions during rainy seasons (Dávila et al. 2007; Vázquez et al. 2014).

Based on the eruptive history here described, four main different eruptive scenarios can be identified: (1) edifice failure; (2) Plinian eruption; (3) dome collapse (Merapi, Soufriere or Vulcanian eruptions); (4) rain-triggered lahars. Here, we present the hazard zonation for

Table 1 Edifice collapse events identified at the Volcán de Colima

Type of material	14C conventional age	Volume (km3)	References
Ligneous charcoal from a DAD	2,505 ± 45	na	Cortés et al. (2005)
Ligneous charcoal at the base of a DAD	3,600 ± 120	1,7	Cortés et al. (2005)
Charcoal from a surge on top of a DAD	4,280 ± 180	10	Luhr and Prestegaard (1988)
Ligneous charcoal at the base of a DAD	7,040 ± 160	18	Komorowski et al. (1997)
Base of a DAD	9,671 ± 88;	3	Komorowski et al. (1997), Cortés et al. (2005)
Charcoal form a surge on top of a DAD	9,370 ± 400	10–20	Robin et al. (1987)
Pyroclastic sequence on top of a DAD	13,585 ± 135	1,3	Roverato et al. (2011)
Wood within a DAD	14,690 ± 105		Cortés et al. (2005)
Ligneous charcoal at the base of a DAD (SW)	21,545 ± 265	na	Komorowski et al. (1997)
Paleosol on top of a DAD (SE)	23,890 ± 1,000	1	Roverato et al. (2011)
Paleosol on top of a DAD (SE)	24,450 ± 1,085	na	Komorowski et al. (1997)

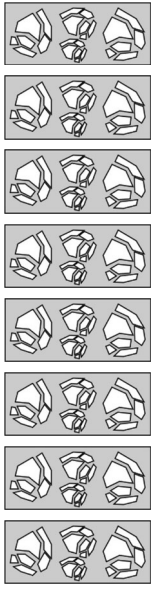

each of these different scenarios and a final qualitative hazard map from the superimposition of the different maps, highlighting the most exposed areas to volcanic hazards at Volcán de Colima. Even if lava flow occurred during the last decades during exogenous event of lava dome growth, they are not considered here in the hazard evaluation since they are limited to few km from the source. Only Navarro and Cortés (2003) reported the lava flow hazard zonation in their map, but simply depicting the extension of past lava flows.

3 Hazard zonation maps

3.1 Edifice failure scenario (debris avalanche and associated secondary debris flow)

Edifice failure can be considered a common occurrence at Volcán de Colima when compared with other Mexican stratovolcanos (Capra et al. 2002b). Based on the stratigraphic record, these collapses were accompanied by explosive activity, as testified by the presence of pyroclastic layers in direct contact with the debris avalanche deposits (i.e., Komorowski et al. 1997; Cortés et al. 2010b; Luhr et al. 2010; Roverato et al. 2011). The structural regime acting on the volcano, with a N–S component of the maximum horizontal stress and coupled with a spreading effect to the south, has been also considered as a controlling parameter of the volcano instability (Norini et al. 2010). The studied events indicate that the volcano experienced different flank failures with volumes between 1 and 2 km^3, and major sector collapses with volumes up to 18 km^3 (Table 1). Based on a statistical analysis of the events occurred during the Holocene, Borselli et al. (2011) recognized a possible recurrence time of 2,698 years, suggesting that the next collapse could happen in $\sim$300 years from present. Borselli et al. (2011) also defined that, at present, the more instable portion of the volcano is the SW flank, with an involved mass of around 1 km^3, used to simulate inundation limits with the Titan 2D code (Borselli et al. 2011). This scenario represents a good estimation of a possible flank failure, and here it is used to define the hazard zonation (Fig. 2). For sector collapses of larger volume, in the range of 5 km^3, which would correspond to the total collapse of the active Volcán de Fuego cone (calculated from an altitude of 2,700 m a.s.l. up to its summit), the hazard zonation is based on the distribution of debris avalanche deposits as observed in the field (Cortés et al. 2010a). Even if deposits of larger volume have been reported (Stoopes and Sheridan 1992; Komorowski et al. 1997; Table 1), they are not realistic due to the actual volume of the Volcán de Fuego cone. Most of the past events were associated to explosive eruptions, and diluted (blast) and concentrated PDC deposits were described on top of debris avalanche deposits (Komorowski et al. 1997; Cortés et al. 2010b; Roverato et al. 2011). We are not able to propose a hazard zonation for such a type of phenomena, since field data on maximum runout are very scarce, but they should be taken into account in case of the occurrence of an edifice failure. Moreover, it is worth mentioning that concentrated PDCs will affect the area already devastated by the debris avalanche itself (i.e., 1980 Mt St Helens eruption, i.e., Waitt 1981). A further complication, as indicated by past events, is that debris avalanche deposits are able to reach the two main rivers that flank the volcano, Naranjo and Armería. The avalanche deposits can dam the river flows, inducing the formation of temporary lakes whose failure would generate large debris flows of the order of 0.1 km^3 (Capra and Macías 2002; Cortés et al. 2010b). In order to take into account this eventuality, the hazard zonation (Fig. 2) includes inundation limits for debris flows on these rivers based on LAHARZ simulations (Schilling 1998), including the

Table 2 Chronology of the eruptive history of the Volcán de Colima during the last ~500 years

Year	Type of activity	Observation	References
1519–1523	Explosive activity		Clavijero (1974[1780])
1560	Data unavaible		Medina-Martinez (1983), De la Cruz-Reyna (1993)
1576	Vulcanian	Strong explosion and associate seismic activity	Arreola (1915)
1585	Probable Sub-Plinian	Seismic activity associated, ash fall up to 220 km, pyroclastic flow on SW	Arreola (1915)
1590	Undefined explosive activity	Ash fall	Orozco and Berra (1888), Waitz (1915)
1602	Strong fumarolic activity		Portillo (1947)
November 9, 1606	Vulcanian	Ash fall and gas emission	
December 13, 1606	Vulcanian	Ash fall up to 200 km from the volcano toward NE up to Zacatecas town; pyroclastic flow on the SWS sector	Arreola (1915), Medina-Martinez (1983)
April 15–20, 1611	Vulcanian	Ash and scoria fall	Tello (1651), Waitz (1915), Medina-Martinez (1983)
1612–13	Strong explosions	Intense seismic activity	Waitz (1932)
June 8–9, 1622	Probable Sub-Plinian	Ash fall up to 400 km from the volcano	Tello (1651), Orozco and Berra (1888)
1690	Strong explosions (pelean)		Medina-Martinez (1983)
1711	Sub-Plinian	Ash fall up to Guadalajara, 140 km NNE from the volcano	Puga (1889–1890)
1744	Persistent explosion	Ash fall in Colima town and lahars	AGI (744)
March 10, 1770	Strong Explosions (probable sub-Plinian)	Several pyroclastic flows that induced fires and cattle deaths toward the S; ash fall toward N up to 550 km	BNM (1789)
March–September, 1795; 1804–1807–1808	Explosions accompanied by effusive activity		AGN (1795), Arreola (1915)
February 15, 1818	Plinian	Ash fall toward NE up to 470 from the volcano, roofs collapses at Zapotlan town, 30 km NE from the volcano. Pyroclastic flow on the SE slope of the volcano; strong explosions heard up to 250 km of distance from the volcano	Barcena (1887), Orozco and Berra (1888), Luhr and Carmichael (1990)
March 1866	Effusive	Extrusion of lava that overflowed the crater rim	Barcena (1887), Medina-Martinez (1983)

Table 2 continued

Year	Type of activity	Observation	References
From June 12, 1869, 1872, 1875–1878	Fissural activity forming the Volcancito cone	Pyroclastic fall and lava flow from a fissure on the NE flank of the volcano forming a small cone; lava flow toward the N on the El Playón area, eruptive columns up to 4,000 m in height	Barcena (1887), Arreola (1915), Waitz (1932), Luhr and Carmichael (1990)
1886	Several vulcanian explosions	Ash fall in Colima town	Barcena (1887)
1889	Vulcanian eruption	Pyroclastic flow, ash fall up to 1,220 m NE from the volcano	Arreola (1915), Medina-Martinez (1983)
1898–1902	1,000 small explosions	Ash fall in the proximity of the volcano	Diaz (1906)
February–March, 1903	Strong explosions	Rising columns (up to ~6,000 m), ballistic projectiles, heavy ash fall on Zapotlan, and up to 200 km NE from the volcano	Arreola (1915), Ordóñez (1903), Starr (1903)
1904–1906	Fumarolic activity, dome growing	Small rock fall from growing lava dome	Diaz (1906), De la Cruz-Reyna (1993)
1908–1909	Small explosion		Waitz (1932)
January 20, 1913	Plinian eruption	January 18–19: phreatic explosions. On January 20 strong explosions with a 23 km column high, ash fall up to 700 km from the volcano	Waitz (1932), Ortiz (1944), Saucedo et al. (2010)
1914–1960	Low level of activity	Some lava reported into the crater, vapor emission	Zehle (1932), Sosa (1952)
1957–1960	Dome grow	Lava dome, on March 2060, the lava overcome the northern rim	Mooser (1961)
1961	Lava flow	Lava flow on the N reaching the flow of the El Playon depression	Mooser and Maldonado-Koerdell (1963)
1966/1967/1973	Minor explosion	Fumarolic activity, rock fall from the summit dome	Medina-Martinez (1983)
1975	Lava flow	Explosion accompanied the extrusion of a new blocky lava toward NE and SE, up to 3.5 km	Thorpe et al. (1977)
1981	Lava dome	Explosions accompanied the emplacement of a new dome and extrusion of blocky lava flow on the SE and S up to 1 km	Smithsonian Institution (1982)
1987/88	Dome grow/collapse	Merapi-type explosions	Smithsonian Institution (1987, 1988)

Table 2 continued

Year	Type of activity	Observation	References
April 16, 1991	Dome grow/collapse	Merapi time activity with the emplacement of PDC toward the SW. On April 20, a blocky lava flow emplaced on the same direction up to 3 km	Rodriguez-Elizarraras et al. (1991)
1994	Dome explosion	Phreatic explosions destroyed the summit dome producing PDC on main ravines	Smithsonian Institution (1994,1995)
1998–1999	Dome grow/collapse	Dome extrusion that overcomes the crater on the SW side originating PDC	Navarro-Ochoa et al. (2002)
1999	3 strong vulcanian explosions	8,000 m high columns, PDC on main ravine, and ash fall up to 20 km toward W. Hot lahars	Smithsonian Institution (1999), Macías et al. 2006
2004–2005	Dome grown/ destruction	Dome extrusion. Merapi- and Soufriere-type activity generating PDC on main ravines up to 6.1 km form the summit	Smithsonian Institution (2004, 2005), Macías et al. (2006), Gavilanes-Ruiz et al. (2009), Sulpizio et al. (2010)
2007–2012	Dome growth	Extremely slow dome extrusion, accompanied by small vapor explosions	Smithsonian Institution (2007,2011), Gavilanes-Ruiz and Cuevas-Muñiz (2014) in press

possible extension of temporary lakes, estimated considering a maximum debris avalanche thickness of 80 m into the river flows (Cortés et al. 2010b).

3.2 Plinian eruptive scenario

The AD 1913 eruption has been classified as VEI 4 (Saucedo et al. 2010; Bonasia et al. 2011), and based on a statistical analysis, the probability of occurrence of at least one eruption exceeding a VEI 3 over a time period of 100 years is 0.8 (Mendoza-Rosas and De la Cruz-Reyna 2008).

The AD 1913 eruption occurred after one decade of low activity (Table 2), and started on January 18, with an opening phase producing gravitation collapse of the summit dome and forming block-and-ash flows that reached a distance down to 4 km from the summit. On January 20, a second eruptive phase started with strong Vulcanian explosions generating block-and-ash flow deposits with up to 20 % of scoria fragments that extended down to 12 km from the crater. After less than 2 h, the paroxysmal phase took place and an eruptive column of 23 km in height formed, lasting 9 h. Stratospheric winds dispersed the tephra to the NW, and ash deposition has been reported as far as on Saltillo city, 700 km away from Volcán de Colima (Saucedo et al. 2010). During the Plinian column formation, partial collapses emplaced pumice/scoria-rich PDCs on main ravines down to 15 km from the vent. A dilute PDC preceded the column formation, and its deposits have been recognized

Fig. 2 Hazard assessment for edifice failure (1 and 5 km^3) and associated secondary effects such as debris flow from dam-break ▶

up to the north flank of Nevado de Colima volcano, just at the base of the fallout layer (Saucedo et al. 2012). Based on the direct observation of the AD 1913 activity, two major hazards have to be considered during Plinian activity: fallout and PDC generation.

3.2.1 Fallout deposits

Bonasia et al. (2011) reconstructed the Plinian phase of the 1913 eruption and constrained the volcanological parameters applying a best-fit inversion method using field data measured by Saucedo et al. (2010). The obtained values for total mass and column height, together with a statistical set of re-analysis wind profiles, were used as input parameters for the HAZMAP code (Macedonio et al. 2005) to construct tephra loading probability maps for two different thresholds (100 and 200 kg/m^2) which, considering a deposit density of about 1,000 kg/m^3 (typical for basalt-andesite fallout deposit), correspond to a thickness of 10 and 20 cm, respectively. These ash loading thresholds are considered critical for low to medium quality buildings. Based on these maps we selected the 1 and 10 % probability curves of exceeding a deposit thickness of 10 cm. Its oblate shape reflects seasonal changes in wind direction (Fig. 3).

3.2.2 Column collapse-generated PDCs

Saucedo et al. (2005, 2010) evaluated the distribution and maximum extent of PDCs originated during the Plinian phase of the AD 1913 eruption, and proposed the hazard zonation based on H/L estimation and using the FLOW3D code. They proposed three different hazard zonations for PDCs generated by Merapi-type dome collapse, Vulcanian activity and partial collapse of the Plinian eruptive column. The Merapi type, along with moderate Soufriere-type activity represents a very common eruptive style at Volcán de Colima during dome grown episodes. These eruptive scenarios have been recently evaluated by Sulpizio et al. (2010) and they will be described in the next paragraph. The work published by Saucedo et al. (2005) represents the only effort to analyze the hazard related to strong Vulcanian explosions and partial column collapse producing block-and-ash flows with a content up to 20 % of juvenile fragments (pumice and scoria) and pumice/scoria flow, respectively. This zonation is here used and it shows that main ravines will be filled with dense material down to distances of 15 km from de source (Fig. 3). A major problem is to define the possible extent of the ash cloud accompanying dense PDCs, from which ash fall or dilute PDCs can originate (e.g., Sulpizio et al. 2014). For this purpose and based on direct observation just after the AD 1913 eruption, an energy cone with a H/L value of 0.2 was used to trace the possible limit of affectation. Even if this approach defines only a rough approximation, the area enclosed on the H/L = 0.2 line is in agreement with the observed field data, and it was modified to the north to consider the extent of the surge deposit as observed at the base of the pumice fall layer near the summit of the Nevado de Colima edifice (Saucedo et al. 2012).

3.3 Dome collapse

During the last 20–30 years, the eruptive activity of Volcán de Colima has been characterized by repetitive growth and collapse of summit domes, which generated block-and-ash

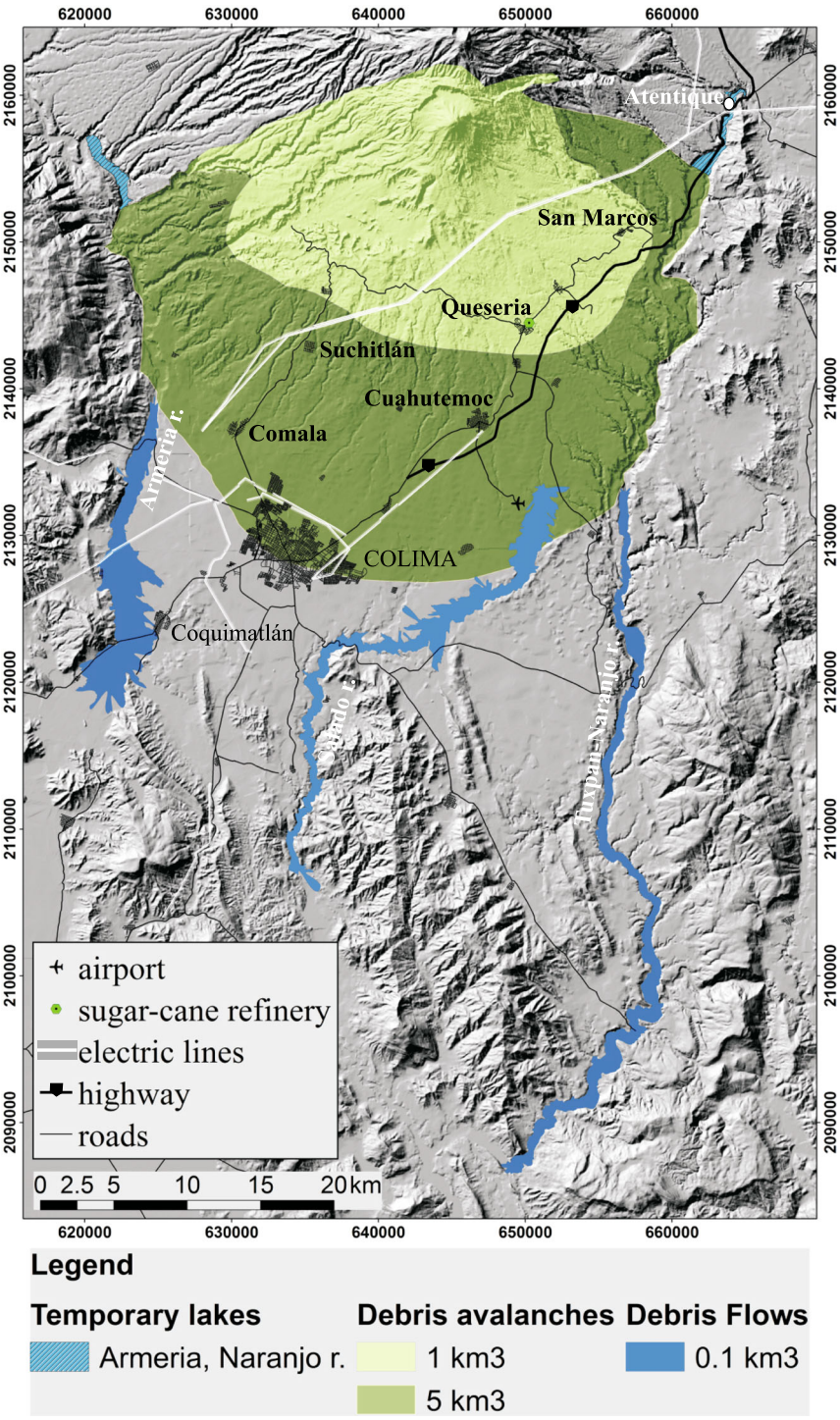
620000
630000
640000
650000
660000
2160000
2150000
2140000
2130000
2120000
2110000
2100000
2090000
Atenticique
San Marcos
Queseria
Suchitlán
Cuahutemoc
Comala
COLIMA
Coquimatlán
Armeria r.
Naranjo r.
airport
sugar-cane refinery
electric lines
highway
roads
0 2.5 5 10 15 20km
Legend
Temporary lakes
Armeria, Naranjo r.
Debris avalanches
1 km3
5 km3
Debris Flows
0.1 km3

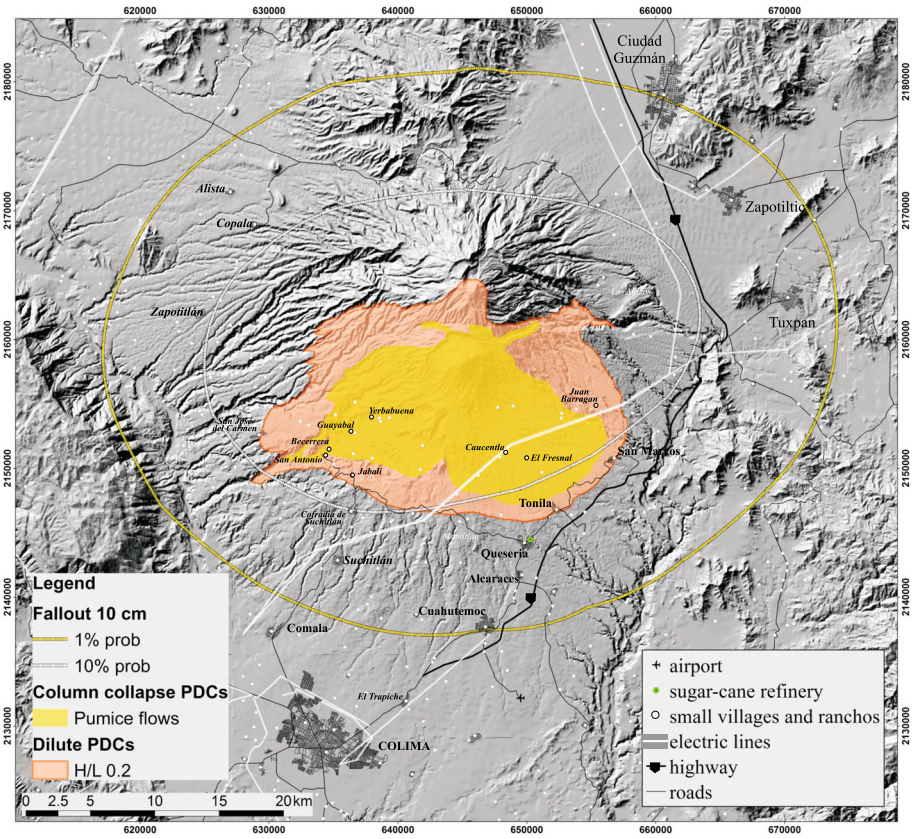

Fig. 3 Hazard assessment for Plinian eruption, including distribution of column collapse pumice flow deposits, dilute pyroclastic density current (H/L 0.2), 10 cm fallout probabilistic curves (1 and 10 %)

flows that inundated the upper slopes of the volcano and engulfed the deep and incised valleys at the base of the main cone. The last major block-and-ash flow-generating explosion occurred in June 2005 (Macías et al. 2006). It closed the 2004–2005 period of activity of the volcano and completed the dismantling of the summit dome. Since early 2007, a new dome has slowly grown in the funnel-shaped crater on the volcano summit (Stevenson and Varley 2008). Two main dome collapse behaviors have been recognized, gravitational (Merapi type) and explosive (Soufriere type). Gravitational dome collapses generated BAF deposits mostly on the SW ravines, down to 4 km of distances, except for the AD 2004 event that generated a BAF along the La Lumbre ravine down to 6.1 km from summit cone. In contrast, dome explosions generated more mobile block-and-ash flows along all main ravines, which easily reached distances down to 5.5 km from the source. No stronger Vulcanian explosions generating longer runout (>10 km) of BAFs such as those reported during the 1913 have been observed during these dome growth episodes. Sulpizio et al. (2010) proposed a hazard zonation for both Merapi- and Soufriere-type dome collapses, including the possible extent for ash cloud deposition accompanying the dense basal avalanche estimated with a H/L of 0.3 (Fig. 4).

3.4 Rain-triggered lahars

Lahars are very common occurrences at Volcán de Colima, including events that followed major edifice failure (Cortés et al. 2010b; Roverato et al. 2011) and Plinian activity (Saucedo et al. 2010). More commonly, they are initiated by heavy rains that occur each rainy season (from June to October), being more voluminous in correspondence of hurricanes or very extreme rain events (Capra et al. 2013, 2014). Rain-triggered lahars are very variable in volume, from a minimum of 3×10^5 m^3 (Dávila et al. 2007; Capra et al. 2010; Vázquez et al. 2014) to 3×10^6 m^3, which corresponds to the extraordinary event occurred in AD 1955 (Saucedo et al. 2008). This event was originated on the SE slope of Nevado de Colima, where several discrete pulses combined to form the main debris flow in the Atenquique main drainage, killing 23 people in the homonymous village and emplacing a 3.2×10^6 m^3 deposit as far as 25 km from the source, reaching also the Tuxpan River (Saucedo et al. 2008). After the AD 1913 Plinian eruption, several lahars occurred along main ravines and reached distances as far as 20 km from the summit cone, where they diluted into the Tuxpan River. No volume estimations are available for these events, but their runout is of the same order of magnitude of that of the Atenquique event (Saucedo et al. 2008). Based on LAHARZ simulation (Schilling 1998), Dávila et al. (2007)

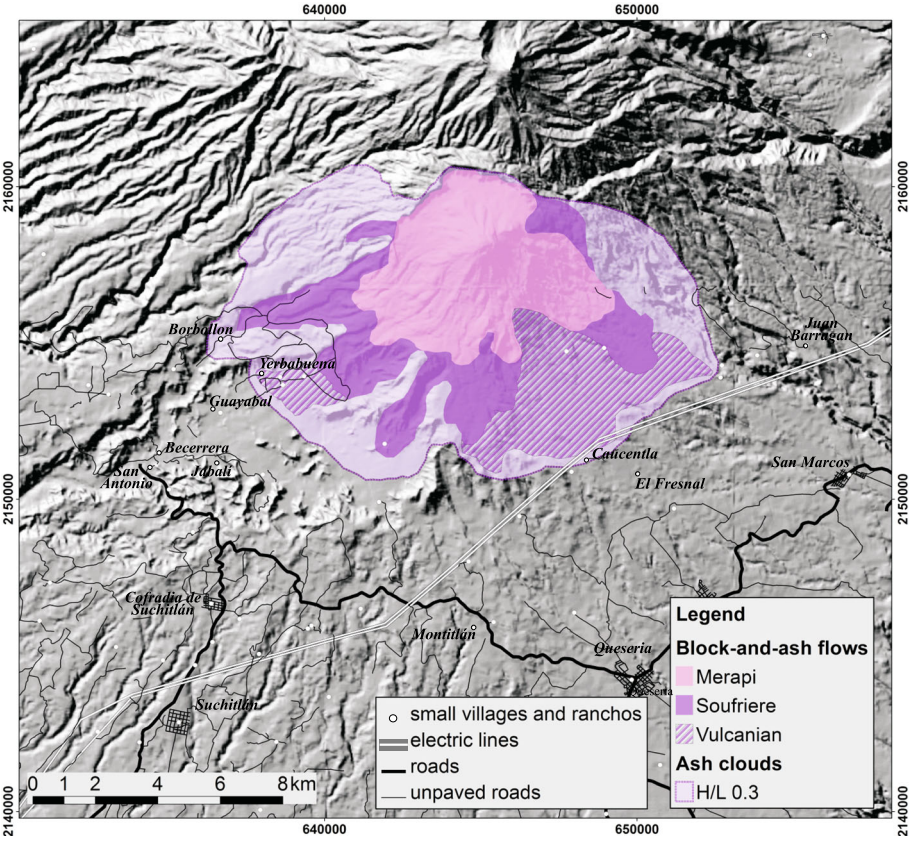

Fig. 4 Hazard assessment for summit dome collapse, including Merapi-, Soufriére- and Vulcanian-type eruptive scenarios and possible extension of the ash cloud inundation zone (H/L 0.3)

performed the hazard evaluation for a low volume (0.5×10^6 m^3) rain-triggered lahars along main ravines (Fig. 5). The same methodology was used for lahars with a volume of 5×10^6 m^3, value that includes events such as the AD 1955 Atenquique episode or the post-eruptive lahars that followed the AD 1913 Plinian eruption that were able to reach the two main rivers in the area, the Armería and Tuxpan-Naranjo (Gavilanes-Ruiz 2004; Capra et al. 2014).

4 Discussion: qualitative hazard map

Based on the single eruptive scenarios presented in the previous sections, we propose here a map comprehensive of all different type of activities (Fig. 6). Since no probability of occurrence is here defined, this map represents a qualitative hazard map where maximum extent of the areas that can be affected by different eruptive scenarios is defined. Edifice failures represent the major hazard for the southern sector of the volcano. A discrete flank failure (~ 1 km^3) would threat an area included in a radius of 20 km from the volcano summit, filling major ravines where subsequent lahars will form reaching the Armería and Tuxpan-Naranajo Rivers. In case of the more voluminous sector collapse (5 km^3), the southern region of the volcano, down to more than 40 km from the summit, would be

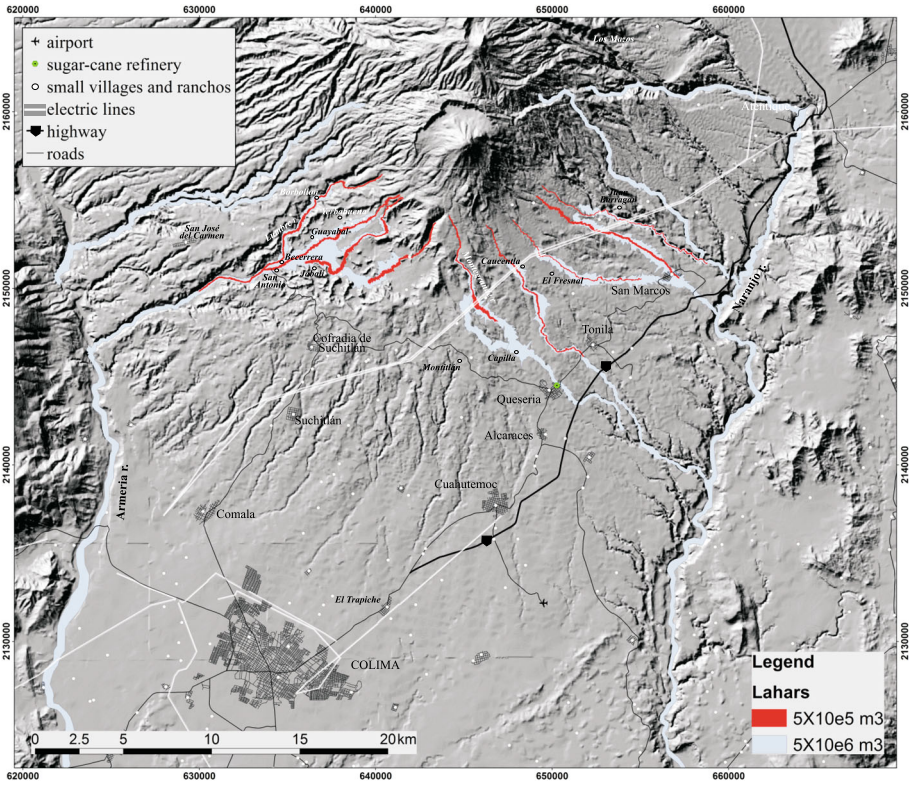

Fig. 5 Hazard assessment for post-eruptive rain-triggered lahars (5×10^5 m^3) and syn-eruptive episodes (5×10^6 m^3) such as those associated to the 1913 Plinian eruption

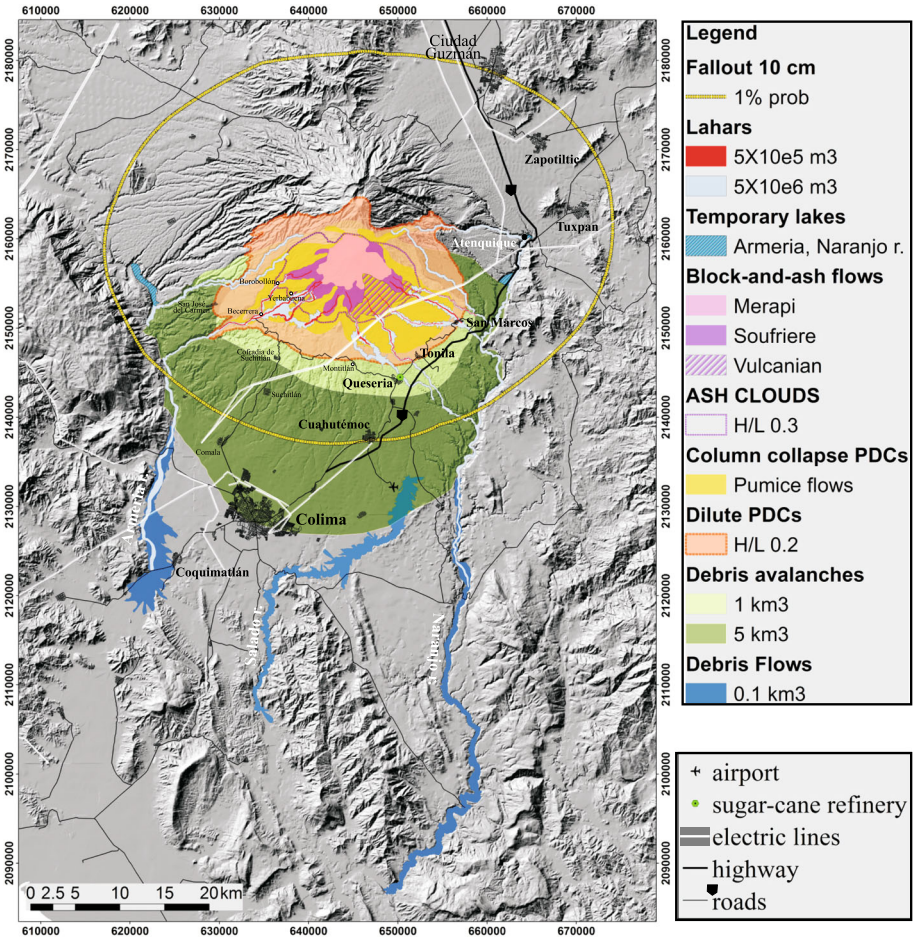

Fig. 6 Qualitative volcanic hazard map of the Volcán de Colima

affected and buried, directly threatening more than 300,000 people and including the Colima city. In addition, the emplacement of the debris avalanche deposits in Naranjo and Armería rivers would induce the formation of temporary lakes, whose ruptures would trigger voluminous debris flows that would inundate areas far away from the volcano, reaching the Pacific coast. Based on the evidences of past events, edifice collapses were associated with magmatic activity with high probability to be accompanied by a blast (Belousov et al. 2007).

The fallout hazard zonation covers a wide area. The lower probability curve (1 %) of exceeding a deposit thickness of 10 cm could affect an area of 535 km^2, including several towns ($\sim$180,000 of inhabitants) such as Cuahutémoc, San Marcos, Zapotiltic, Tuxpán and Ciudad Guzmán where, during the AD 1913 eruption, 10–13 cm of ash were reported (Saucedo et al. 2010). The Colima city is outside of this hazard zonation, which indicates that it could be affected by less than 10 cm of ash due to stratospheric wind direction in the area (mainly to N, NE or NW). The Colima national airport located near Cuahutémoc town would also suffer from the presence of ash in the atmosphere, with interruption of flight

Fig. 7 **a** Volcanic susceptibility map of the Volcán de Colima based on a simple raster operation to identify the areas that are exposed to the highest number of events. **b** Classified volcanic susceptibility map to identify the areas with different level of hazards. The table indicates the number of inhabitants that can be affected for each level of hazard (demographic data from INEGI, 2010)

operations. Apart from the possible damage to infrastructure, heavy ash fall would threat all the cultivated areas that are extensively distributed on the volcano slopes, with severe loss for the sugarcane industry, which is located in Quesería village (Fig. 6). It is important to take into account that, in case of lower eruptive columns, winds can probably disperse ash to the S, as occurred on AD 2003, after a strong Vulcanian explosion, or as reported in the historic record (Table 2). Even in that case, reduced amount of ash would settle in Colima city.

PDCs associated to Plinian or sub-Plinian eruptions and strong Vulcanian explosions can affect several villages in a radius of 15 km from the summit cone. Column collapse-generated PDCs would fill major ravines, with the possibility to affect la Yerbabuena (evacuated during the AD 1999 and AD 2002 volcanic crises), Becerrera, Tonila and San Marcos villages, for a total of more than 7,000 of inhabitants including several ranches. In particular, the southern sector of the volcano is largely cultivated for sugarcane, and during daytime, tens of workers are dispersed on these fields, especially on the S-SE sector. Finally, lahars along the Monte grande ravines would be able to damage the sugarcane refinery at Quesería town. BAFs from dome collapse are threatening a more reduced area, down to a distance of 8 km from the crater. The dense basal avalanche would be confined to major ravines, without direct affectation of inhabited areas. In contrast, the ash cloud would be able to affect a larger area overrunning topographic highs, as observed in other volcanoes (Merapi, Indonesia, Itoh et al. 2000; Unzen, Japan, Fujii and Nakada 1999) provoking deaths and injuries in up to five ranches, including El Borbollón, located besides La Lumbre ravine. Finally, lahars, with variable magnitude, can inundate main ravines, with major damage to towns that are settled along active drainages such as Atenquique, San Marcos and Quesería (Fig. 1d). The new map here proposed differs substantially from the previous published maps (Navarro and Cortés 2003; Del Pozzo et al. 1996), since it includes the hazards zonation for different types of PDCs related to different eruptive scenarios, lahars and debris avalanche inundation areas depending on the flow volumes, and ash fall distribution based on a statistical evaluation of wind direction. In addition, secondary effects such as the formation of temporary dam along the main rivers are also included. Based on these scenarios, a susceptibility map is presented, showing the most exposed areas to volcanic threat. The map was constructed by a simple arithmetic sum of rasters of all hazard zonation previously described, to obtain the maximum number of event that affects each pixel (Fig. 7a). The sector collapse of the active cone (5 km^3) is not here considered since at present does not represent a realistic scenario and in case of occurrence it will affect all the area (Fig. 6). The map was then classified in four main levels of hazards (Fig. 7b) based on the combination of different hazardous occurrences that can affect a given area (Bartolini et al. 2014). The high-level area extends down to 8.5 km from the crater, and it is exposed to all of the considered hazardous events. In particular, it corresponds with the area that can be affected by PDCs from Merapi- and Soufriere-type dome collapse, and lahars ($<5 \times 10^5$ m^3) along main ravines. These episodes represent the most common and frequent eruptive scenarios of dome collapses and rain-triggered lahars as observed during the last 20 years (Table 2). The moderate-level includes the area from 8.5 to 12 km from the vent and corresponds to the emplacement

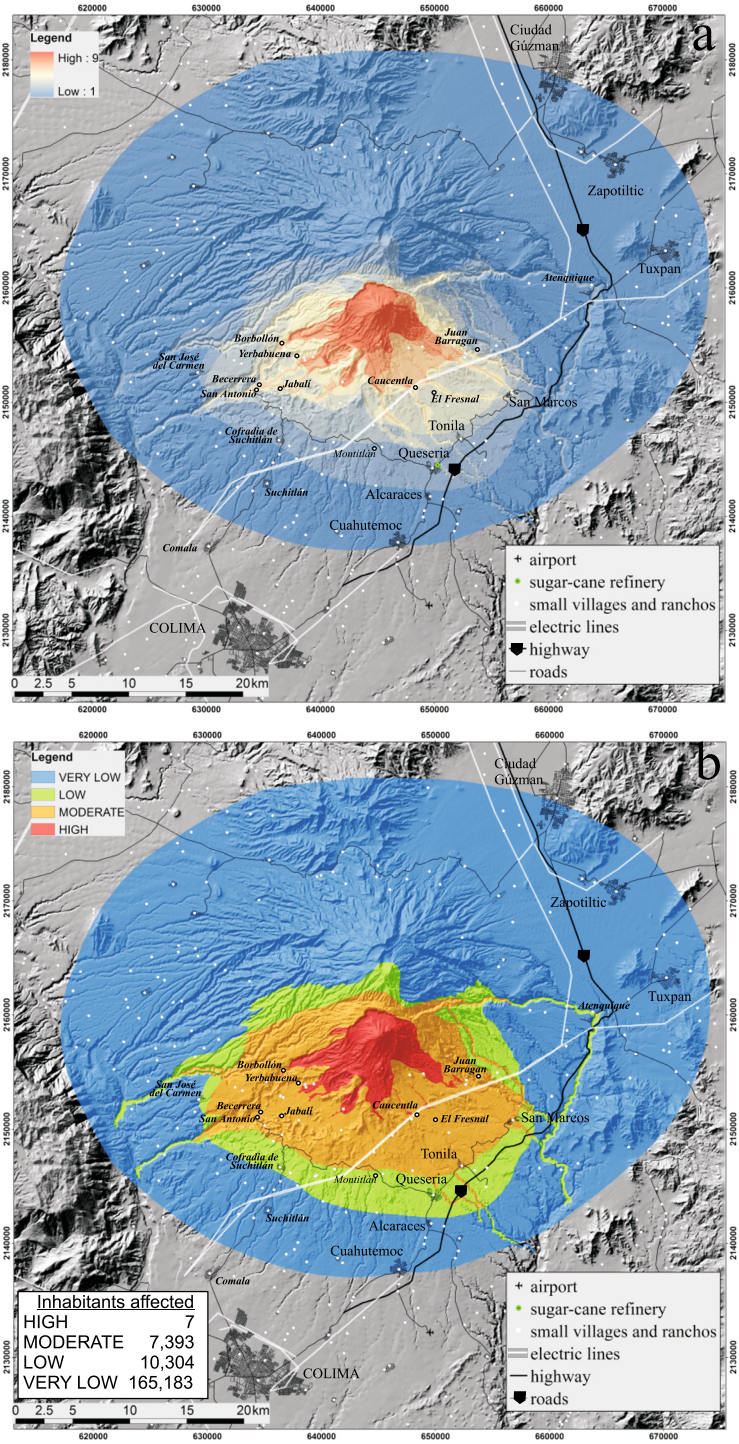
a
Legend
High : 9
Low : 1
Ciudad Guzman
Zapotiltic
Tuxpan
Atenquique
Borbollón
Yerbabuena
Juan Barragan
San José del Carmen
Becerrera
San Antonio
Jabalí
Caucentla
El Fresnal
San Marcos
Tonila
Cofradia de Suchitlán
Montitlán
Queseria
Suchitlán
Alcaraces
Cuahutemoc
Comala
COLIMA
airport
sugar-cane refinery
small villages and ranchos
electric lines
highway
roads
0 2.5 5 10 15 20km
b
Legend
VERY LOW
LOW
MODERATE
HIGH
Inhabitants affected
HIGH 7
MODERATE 7,393
LOW 10,304
VERY LOW 165,183

area of PDCs associated to strong Vulcanian explosions and associated ash clouds (H/L = 0.3), PDCs from Plinian column collapses and associated ash cloud (H/L = 0.2), including more than 10 cm of fallout and lahars (>5 × 10^6 m^3). This eruptive scenario corresponds to the Plinian phase of the AD 1913 eruption (Saucedo et al. 2010) and represents a threat for more than 7,300 of people. The low-level zone includes the area that could be affected by debris avalanches from flank collapses (1 km^3), more than 10 cm of fallout, and dilute PDCs on top of the Nevado de Colima volcano. Finally, the very low-level correspond with the rest of the area that can be threatened by more than 10 cm of fallout, which can cause several damage to infrastructures at several towns (∼160,000 of inhabitants) such as Tuxpan and Ciudad Gúzman as occurred during the 1913 Plinian eruption. This type of map could be considered as a qualitative volcanic hazard map, which can be useful to Civil Protection authorities in defining different actions depending on the most probable eruptive scenario during a volcanic crisis. The classified map could be used to establish different level of volcanic alert, such as the system used at Popocatépetl volcano, where a "traffic light" with three main phases as green, yellow and red, and each of them with different sub levels is considered for alert purposes (Centro Nacional de Prevención de Desastres, http://www.cenapred.gob.mx/es/Instrumentacion/InstVolcanica/MVolcan/Semaforo/).

5 Conclusion

A qualitative volcanic hazard map that shows the area exposed to the highest number of volcanic events is proposed. The hazard map poses in evidence that an eruption of VEI 4, such as the 1913 Plinian eruption, would cause serious consequences not only for the areas directly exposed to the impact of pyroclastic flows and lahars, but for a larger area that can be covered by pumice and ash fall with direct affectation on transportation (terrestrial and aerial), communication, lifelines, agriculture and health for more than 300,000 people, including the cities of Colima and Villa de Alvarez. Commercial activities of the western portion of México would also suffer economic losses since the highway N.54 (Fig. 6), an important connection between the cities of Guadalajara and Manzanillo, being the last the most important harbor of the Pacific Mexican coast, would be affected by the ash fall. In contrast, the most common scenario is restricted to the proximal area with local effects on small ranches and people working in the field. The most catastrophic effect would be related with the flank collapse of the volcano, which represents the less frequent eruptive scenario, but that can cause, in case of occurrences, devastating effects.

The hazard assessment here presented may help decision makers during volcanic crises in defining risk mitigation actions such as evacuation to reduce the loss of life due to the potential impact of volcanic hazards. A study performed by Gavilanes-Ruiz and Cuevas-Muñiz (2014), applied to some inhabitants of the most threatened villages, showed that their knowledge and wisdom regarding the general features of the volcanic activity and hazards are not in contrast to those of authorities and earth scientists. In fact, they generally recognize the lethal power of the volcano, but many of them simply have not found sufficient reasons to participate in evacuations (Gavilanes-Ruiz and Cuevas-Muñiz 2014). Even though the increased public knowledge about volcanic risk does not guarantee the willingness to participate in official risk mitigation strategies, the same studies indicated that the information and risk communication programs as the one performed during 1997–2000 (including the explanation of hazard zoning) improve risk perception and thus should be continued in order to achieve a long lasting impact.

Acknowledgments This work was supported by CONACyT 99486 and 46304, PAPIIT-UNAM IN-106710 and IN103107, SRE-CONACYT 146324 projects to Lucia Capra. Thanks to Penelope López to manage Spot image acquisition from ERMEXS- SPOT IMAGE, S. A. Comments from Gianluca Groppelli and an anonymous reviewer greatly improuved the manuscript.

References

AGI (Archivo General de Indias) (1744) Indiferente General 107: 250–255

AGN (Archivo General de la Nacion) (1795) Real Hacienda 829: file 129

Arreola JM (1915) Catálogo de las erupciones antiguas del Volcán de Colima. Mem Rev Soc Cient 32:443–481 Antonio Alzate, Mexico

Barcena M (1887) Informe sobre el estado actual del Estado de Colima. In: El Estado de Colima. Periodico Oficial del Gobierno, vol. XXI, no. 2, January

Bartolini S, Geyger A, Martí J, Pedrazzi D, Aguirre G (2014) Volcanic hazard on Deception Island (South Shetland Islands, Antarctica). J Volcanol Geotherm Res 285:150–168

Belousov A, Voight B, Belousova M (2007) Directed blasts and blast-generated pyroclastic density currents: a comparison of the Bezymianny 1956, Mount St Helens 1980, and Soufrière Hills, Montserrat 1997 eruptions and deposits. Bull Volcanol 69(7):701–740

BNM (Biblioteca Nacional de Madrid) (1789) Manuscript 2450, No. 86: 146–149

Bonasia R, Capra L, Costa A, Macedonio G, Saucedo R (2011) Tephra fallout hazard assessment for a Plinian eruption scenario at Volcán de Colima (Mexico). J Volcanol Geotherm Res 203:12–22

Borselli L, Capra L, Sarocchi D, De la Cruz-Reyna S (2011) Flank collapse scenarios at Volcán de Colima, Mexico: a relative instability analysis. J Volcanol Geotherm Res 208:51–65

Breton M, Ramirez JJ, Navarro C (2002) Summary of the historical eruptive activity of Volcán De Colima, Mexico 1519–2000. J Volcanol Geotherm Res 117:21–46

Capra L, Macías JL (2002) The cohesive Naranjo debris flow deposit (10 km3): a dam breakout flow derived from the pleistocene debris-avalanche deposit of Nevado de Colima volcano (México). J Volcanol Geotherm Res 117:213–235

Capra L, Macias JL, Scott KM, Abrams M, Garduño-Monroy VH (2002) Debris avalanche and debris flow transformed from collapses in the Trans-Mexican Volcanic Belt, Mexico—behavior, and implication for hazard assessment. J Volcanol Geotherm Res 113:81–110

Capra L, Borselli L, Varley N, Norini G, Gavilanes JC, Sarocchi D, Caballero C (2010) Rainfall-triggered lahars at Volcán de Colima, Mexico: surface hydro-repellency as initiation process. J Volcanol Geotherm Res 189(1–2):105–117

Capra L, Roverato M, Groppelli G, Sulpizio R, Arámbula-Mendoza R, Reyes G, Lube G, Cronin SJ (2013) Hurricane-triggered lahars at Volcán de Colima: evidences of flow dynamic from monitoring and field survey. Abstract with program. IAVCEI, Kagoshima, Japon

Capra L, Gavilanes-Ruiz JC, Varley N, Borselli L (2014) Origin, behavior and hazard of rain-triggered lahars at Volcán de Colima. In: Varley N, Komorowski JC (eds) Volcán de Colima: managing the threat. Active Volcanoes of the World Series, Springer, Berlin (in press)

Clavijero FX (1974 [1780]) Historia Antigua de Mexico, Porrua, Ciudad de México, 4 vols

Cortés A, Garduño VH, Navarro C, Komorowski JC, Saucedo R, Macías JL, Gavilanes JC (2005) Carta Geológica del Complejo Volcánico de Colima, Geología del Complejo Volcánico de Colima. CARTAS GEOLÓGICAS Y MINERAS 0185-4798 vol 10, Instituto de Geología, UNAM, Ciudad de México

Cortés A, Garduño VH, Macías JL, Navarro C, Komorowski J-C, Saucedo R, Gavilanes JC (2010a) Geological mapping of the Colima volcanic complex (Mexico) and implication for hazard assessment. In: Groppelli G, Viereck L (eds) Stratigraphy and geology of Volcanic areas, Geological Society of America, Boulder CO, special paper 464: 294–246

Cortés A, Macías JL, Capra L, Garduño-Monroy VH (2010b) Sector collapse of the SW flank of Volcán de Colima, México. The 3600 yr BP La Lumbre-Los Ganchos debris avalanche and associated debris flows. J Volcanol Geotherm Res 197:52–66

Dávila N, Capra L, Gavilanes JC, Varley N, Norini G, Gómez A (2007) Recent lahars at Volcán de Colima (México): drainage variation and spectral classification. J Volcanol Geotherm Res 165:127–141

De la Cruz-Reyna S (1993) Random patterns of occurrence of explosive eruptions at Colima Volcano, Mexico. J Volcanol Geotherm Res 55:51–68

Del Pozzo AL, Sheridan MF, Barrera D, Hubp JL, Vázquez L (1996) Mapa de peligros Volcán de Colima. Instituto de Geofísica, UNAM, Mexico

Diaz S (1906) Efemerides del Volcán de Colima según las observaciones practicadas en los Observatorios de Zapotlán y Colima de 1893 a 1905.Imprenta y Fototipia de la Secretaria de Fomento, 199 p
Fujii T, Nakada S (1999) The 15 September 1991 pyroclastic flows at Unzen Volcano (Japan): a flow model for associated ash-cloud surges. J Volcanol Geotherm Res 89:159–172
Gavilanes-Ruiz JC 2004. Simulación de Escenarios Eruptivos del Volcán de Colima y Aportaciones al Plan de Contingencias del Estado de Colima. Masters thesis. Facultad de Filosofía y Letras, Instituto de Geografía, Programa de Posgrado en Geografía, UNAM México, p 123
Gavilanes-Ruiz JC, Cuevas-Muñiz A (2014) Understanding knowledge and oral history for risk management: community of La Yerbabuena, Volcán de Colima, México. Eco-Cultural Adaptations in Volcanic Environments. The University of the Philippines, Center for International Studies, Diliman, p 1–14. in press
Gavilanes-Ruiz JC, Cuevas-Muñiz A, Varley N, Gwynne G, Stevenson J, Saucedo-Girón R, Pérez-Pérez A, Aboukhalil M, Cortés-Cortés A (2009) Exploring the factors that influence the perception of risk: the case of Volcán de Colima, Mexico. J Volcanol Geotherm Res 186:238–252
Institution Smithsonian (1982) Colima. Sci. Event Alert Bull. 7:1–3
Itoh H, Takahama J, Takahashi M, Miyamoto K (2000) Hazard estimation of the possible pyroclastic flow disasters using numerical simulation related to the 1994 activity at Merapi Volcano. J Volcanol Geotherm Res 100(1–4):503–516
Komorowski JC, Navarro C, Cortés A, Saucedo R, Gavilanes JC, Siebe C, Espíndola JM, Rodríguez-Elizarrarás SR (1997) The Colima Volcanic Complex. IAVCEI General Assembly, Puerto Vallarta, Mexico, January 19–24, 1997, Fieldtrip Guidbook, Excursion no 3
Luhr JF, Carmichael ISE (1982) The Colima Volcanic Complex, Mexico: III, ash-and scoria-fall deposits from the upper slopes of Volcán Colima. Contrib Miner Petrol 80:262–275
Luhr JF, Carmichael ISE (1990) Geology of Volcan de Colima. Bol. Inst. Geol. UNAM 107: 101
Luhr JF, Prestegaard KL (1988) Caldera formation at Volcán de Colima, Mexico, by large Holocene volcanic debris avalanche. J Volcanol Geotherm Res 35:335–348
Luhr JF, Navarro C, Savov I (2010) Tephrochronology, petrology and geochemistry of Late-Holocene pyroclastic deposits from Volcán de Colima, Mexico. J Volcanol Geotherm Res 197:1–32
Macedonio G, Costa A, Longo A (2005) A compuetr model for volcanic ash fallout and assessment of subsequent hazard. Comput Geosci 31:837–845
Macías JL, Saucedo R, Gavilanes JC, Varley N, Velasco García S, Bursik MI, Vargas Gutiérrez V, Cortés A (2006) Flujos piroclásticos asociados a la actividad explosiva del volcán de Colima y perspectivas futuras. GEOS 25(3):340–351
Medina-Martinez F (1983) Analysis of the eruptive history of the Volcán de Colima, Mexico (1560–1980). Geofis Int 22:157–178
Mendoza-Rosas AT, De la Cruz-Reyna S (2008) A statistical method linking geological and historical eruption time series for volcanic hazard estimations: applications to active polygenetic volcanoes. J Volcanol Geotherm Res 176:277–290
Mooser F (1961) Los volcanes de Colima. Bol Inst Geol UNAM 61:49–71
Mooser F, Maldonado-Koerdell M (1963) State of the volcanoes—Colima Volcano. Mexican Natl. Rpt. on volcanology, General Assembly IUGG, CA, p 13, 7
Navarro C, Cortés A (2003) Mapa de peligros del Volcán de Fuego de Colima. Universidad de Colima, Observatorio Vulcanológico. Gobierno del Estado de Colima
Navarro-Ochoa C, Gavilanes J, Cortes A (2002) Movement and emplacement of lava £ows at Volcán de Colima, Mexico: Nov. 1998-Feb. 1999. J. Volcanol. Geotherm. Res. 117:155–167
Norini G, Capra L, Groppelli G, Agliardi F, Pola A, Cortes A (2010) The structural architecture of the Colima Volcanic Complex. Journal of Geophysical Research 115:B12209. doi:10.1029/210JB007649
Ordóñez E (1903) Les dernièeres eruptions du Volcan de Colima. Mem. Soc. Cient. Antonio Alzate, Mexico 99–103
Orozco MN, Berra J (1888) Seismologia. Efemerides seismicas mexicanas. Mem Rev Soc Cient Antonio Alzate I:303–541
Ortiz SG (1944) La Zona volcánica Colima del Estado de Jalisco. Publicaciones de la Universidad de Guadalajara, Guadalajara, México
Portillo A (1947) Descubrimientos y exploraciones en las costas de California. Publicaciones de la Escuela de estudios Ispano-Americanos de la Universidad de Sevilla, España, pp 20
Puga GB (1889–1890) La ultima erupción del volcán de Colima. Mem. Soc. Cient. Antonio Alzate, Mexico 3: 97–102
Robin C, Mossand P, Camus G, Cantagrel J-M, Gourgaud A, Vincent PM (1987) Eruptive history of the Colima volcanic complex (Mexico). J Volcanol Geotherm Res 31:99–113

Rodriguez-Elizarraras S, Siebe C, Komorowski JC, Espindola JM, Saucedo R (1991) Field observations of pristine block-and ash-£ow deposits emplaced April 16–17, 1991 at Volcán de Colima, Mexico. J Volcanol Geotherm Res 48:399–412

Roverato M, Capra L, Sulpizio R, Norini G (2011) Stratigraphic reconstruction of two debris avalanche deposits at Colima Volcano (Mexico): insights into pre-failure conditions and climate influence. J Volcanol Geotherm Res 207:33–46

Saucedo R, Macías JL, Sheridan MF, Bursik MI, Komorowski JC (2005) Modeling of pyroclastic flows of Colima Volcano, Mexico: implications for hazard assessment. J Volcanol Geotherm Res 139(1–2):103–115

Saucedo R, Macías JL, Sarocchi D, Bursik MI, Rupp B (2008) The rain-triggered Atenquique volcaniclastic debris flow of October 16, 1955 at Nevado de Colima Volcano, Mexico. J Volcanol Geotherm Res 132:69–83

Saucedo R, Macías JL, Gavilanes JC, Arce JL, Komorowski JC, Gardner JE, Valdéz G (2010) Eyewitness, stratigraphy, chemistry, and eruptive dynamics of the 1913 Plinian eruption of Volcán de Colima, Mexico. J Volcanol Geotherm Res 191:149–166

Saucedo R, Macías JL, Gavilanes-Ruiz JC, Arce JL, Komorowski JC, Gardner JE (2012) Reassessment of the 1913 Plinian eruption of Volcán de Colima. Abstract with program, Cities on Volcanoes 7, Colima, Mexico

Schilling S (1998) LAHARZ: GIS programs for automated mapping of lahar-inundation hazard zones. USGS open-file report: 98–638

Smithsonian Institution (1987) Colima Sci Event Alert Bull 12:7

Smithsonian Institution (1988) Colima Sci Event Alert Bull 13(9):12

Smithsonian Institution (1994) Colima Bull Glob Volcanism Netw 19(6):8

Smithsonian Institution (1995) Colima Bull Glob Volcanism Netw 20(2):6

Smithsonian Institution (1999) Colima Bull Glob Volcanism Netw 24(1):2

Smithsonian Institution (2004) Colima Bull Glob Volcanism Netw 29(5):11

Smithsonian Institution (2005) Colima Bull Glob Volcanism Netw 30(6):2

Smithsonian Institution (2007) Colima Bull Glob Volcanism Netw 32(10):8–9

Smithsonian Institution (2011) Colima. Bull. Glob. Volcanism Netw 36(3):13–15

Sosa AH (1952) Excursión al Cráter del volcán de Fuego de Colima. Bol Soc Mex Geogr Estad LXXIII: 1–3

Starr F (1903) The recent eruptions of Colima. J Geol 11:750

Stevenson JA, Varley N (2008) Fumarole monitoring with a handheld infrared camera: Volcán de Colima, Mexico, 2006–2007. J Volcanol Geotherm Res 177(4):911–924

Stoopes GR, Sheridan MF (1992) Giant debris avalanches from the Colima Volcanic Complex, Mexico: implication for long-runout landslides (>100 km). Geology 20:299–302

Sulpizio R, Capra L, Sarocchi D, Saucedo R, Gavilanes JC, Varley N (2010) Predicting the block-and-ash flow inundation areas at Volcán de Colima (Colima, Mexico) based on the present day (February 2010) status. J Volcanol Geotherm Res 193:49–66

Sulpizio R, Dellino P, Doronzo DM, Sarocchi D (2014) Pyroclastic density currents: state of the art and perspectives. J Volcanol Geotherm Res 283:36–65

Tello FA (1651) Libro segundo de la Cronica Miscelanea en que se trata de la conquista espiritual y temporal de la Santa Provincia de Xalisco en el Nuevo Reino de la Galicia y Nueva Vizcaina y Descubrimiento del nuevo MexicoT, Imprenta de la Republica Literaria, Guadalajara

Thorpe RS, Gibson I, Vizcaino J (1977) Andesitic pyroclastic flows from Colima Volcano. Nature 265:724–725

Vázquez R, Capra L, Caballero L, Arambula R, Reyes-Dávila G (2014) The anatomy of a lahar: deciphering the 15th September 2012 lahar at Volcán de Colima, Mexico. J Volcanol Geotherm Res 272:126–136

Waitt RB (1981) Devastating pyroclastic density flow and attendant air fall of May 18- stratigraphy and sedimentology of deposits. In Lipman PW, Mullineaux DR (eds) The 1980 eruptions of Mount St. Helens, Washington, geological survey professional paper, 439–460

Waitz P (1915) Der gegenwartige Zustand der mexikanischen Vulkanen und die letzte Eruption des Vulkans von Colima. Z Vulkanol 1:247

Waitz P (1932) Datos historicos y bibliograficos acerca del volcán de Colima. Mem Rev Soc Cient Antonio Alzate, Mexico 53:349–384

Zehle W (1932) Neue Quellkuppenbildung in Colima Krater. Z Vulkanol, XIV 240